Permittivity and Loss Characterization of SUEX Epoxy Films for mmW and THz Applications

Seckin Sahin, *Graduate Student Member, IEEE*, Niru K. Nahar, *Senior Member, IEEE*, and Kubilay Sertel, *Senior Member, IEEE*

***Abstract*—We present a systematic characterization of the dielectric permittivity and loss tangent of SUEX dry films for mmW and THz bands. Green and cured SUEX samples of varying thicknesses were studied using two complementary measurement techniques. First, the Nicolson–Ross–Weir technique was used in a two-port TE_{10} waveguide environment for 90–140-GHz and 140–220-GHz bands. The samples were also characterized using a transmission-mode time domain THz spectrometer over the 90-GHz–2-THz band. Real part of permittivity and loss tangent were measured to be 3.08 and 0.057, respectively, for the green SUEX sample. Ultraviolet light curing reduces the permittivity and loss tangent down to 2.86 and 0.020, respectively. SUEX films can be easily laminated onto any substrate, eliminating the spin coating and long process optimizations that are required for conventional liquid resists. As such, SUEX is an easy-to-process alternative to commonly used epoxy-based resists, such as SU-8, while exhibiting similar dielectric permittivity and material losses.**

***Index Terms*—Dry-films, loss tangent, millimeter-wave, Nicholson–Ross–Weir method (NRW), permittivity, spectroscopy, SUEX, SU-8, terahertz, time domain.**

I. Introduction

MATERIALS that lend themselves to lithographic microfabrication, while exhibiting low electromagnetic loss are particularly attractive for the fabrication of mmW and THz waveguides, devices, components, and subsystems. Perhaps more importantly, structural support and packaging materials that exhibit low loss are indispensable for cost-effective realization of integrated high frequency systems, including not only the sensors and transceiver electronics but also the on-chip radiating antennas and arrays. Polymers are a natural, low-cost choice for structural support and packaging of microchips due to their favorable chemical, thermal, and mechanical properties. For example, SU-8, a photo-sensitive epoxy-based polymer, is widely used as a structural support for micro electro mechanical systems (MEMS). Thus, significant literature has been developed on the optimization of SU-8 processing techniques. In addition, SU-8 has also been considered for mmW and THz-frequency applications, and the dielectric properties of SU-8 have been well-studied for these bands (see [1]–[4]). However, SU-8 suffers from key processing challenges, such as adhesion and development problems, as reported in [5]–[9]. The quality of patterned SU-8 layers is highly dependent on the particular process and the reoptimization of process variables is often needed when the condition of tools or the design of the microstructure change. Furthermore, nonuniformities of SU-8 layer across the wafer substantially affect the final device performance. To overcome such manufacturing challenges of liquid epoxy resists, a new line of thick dry resists, SUEX thick dry film sheets, was developed recently by DJ DevCorp [10]. SUEX films are precut to various substrate dimensions and can be made to thicknesses ranging from 100 μm to more than 1 mm [11]. High-aspect-ratio structures, upto 50:1, have been demonstrated using SUEX films as thick as 500 μm [12].

As opposed to spin coating, SUEX films are thermally laminated onto the main substrate, a process that takes only minutes, offering significant utility compared to other materials commonly used in MEMS fabrication. SUEX also exhibits improved transparency, making it more suitable for thick resist applications. Excellent uniformity, resolution, and high quality of sidewalls are all key attributes of SUEX dry films.

Much like SU-8, SUEX can also be patterned using either UV or X-ray lithography or hot imprinting/embossing the surface. Furthermore, SUEX can also be processed as free-standing microstructures or be laminated to the different substrates. Although SU-8 has been utilized as a dielectric material for mmW and THz applications, SUEX is relatively new and its electromagnetic properties have not been studied to date. In this letter, we provide a comprehensive characterization of SUEX material permittivity and loss in the mmW and THz spectrum.

In the following, we report the material characterization of SUEX films using the Nicolson–Ross–Weir (NRW) technique, and the transmission-mode time-domain THz spectroscopy. The NRW approach was used in a TE_{10} waveguide environment, where the measured transmission and reflection coefficient were used to extract the complex permittivity and permeability of the

Manuscript received January 29, 2018; revised May 11, 2018; accepted May 17, 2018. Date of publication May 25, 2018; date of current version July 2, 2018. This work was supported by ONR Program no. N00014-14-1-0810. *(Corresponding author: Seckin Sahin.)*

The authors are with the Department of Electrical and Computer Engineering, The Ohio State University, Columbus, OH 43210 USA (e-mail: sahin.29@osu.edu; nahar.2@osu.edu; sertel.1@osu.edu).

Color versions of one or more of the figures in this letter are available online at http://ieeexplore.ieee.org.

Digital Object Identifier 10.1109/TTHZ.2018.2840518

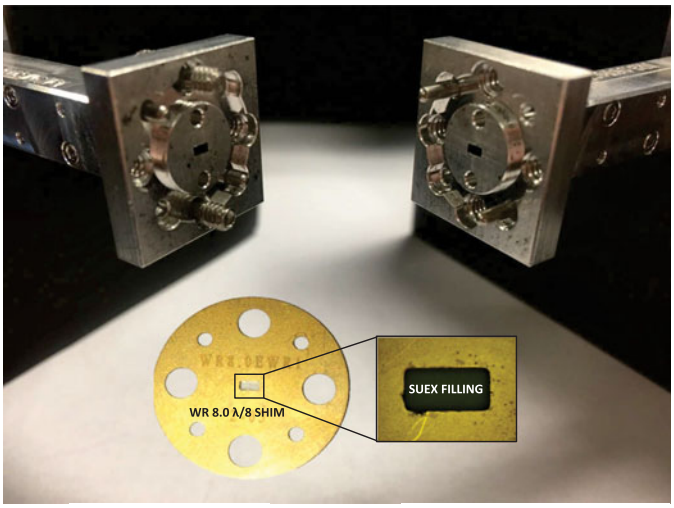

(a)

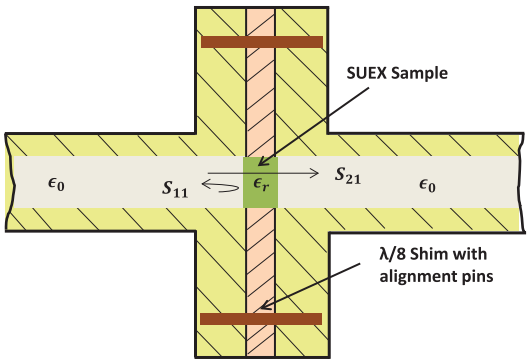

(b)

Fig. 1. Measurement setup. (a) WR 8.0 extensions for 90–140-GHz band along with $\lambda/8$ shim filled with SUEX sample. (b) Schematic diagram of measurement setup.

Fig. 2. SUEX dry film samples, 48-mm diameter with various thicknesses provided by DJ MicroLaminates, Inc.

samples. To do so, the setup in Fig. 1 was used over two successive waveguide bands, namely the 90–140-GHz (WR8.0) and the 140–220-GHz (WR5.1) bands. The results of the NRW technique are also compared with the broadband time-domain THz spectroscopy characterization, where polynomial fitting was used for the real and imaginary parts of the dielectric permittivity over the 90-GHz–2-THz band. The NRW results are consistent with the characterization data using the THz-TDS system.

The paper is organized as follows. Material preparation and experimental setup of the NRW measurement are given in Section II. Next, a summary of the THz-TDS characterization is provided in Section III. The results are summarized and compared in Section IV, with key observations drawn in Section V.

II. NRW Setup for Permittivity Characterization

The NRW technique is based on two-port measurements, where the transmission and reflection coefficients from the sample under test are used to analytically extract the material properties. This approach is quite general, and can be readily applied to rectangular waveguides, as shown in Fig. 1, where the sample is fitted inside the waveguide with one of its faces situated at the calibration plane of Port 1. In our measurement setup, we used an Agilent N5242A PNA-X network analyzer with Virginia Diodes Inc., frequency extenders attached to each port. As mentioned above, we studied two successive waveguide bands, namely WR8.0 and WR5.1, using the available instrumentation. The waveguide dimensions for the aforementioned WR bands are 2.032 mm $\times$ 1.016 mm and 1.2954 mm $\times$ 0.6477 mm, respectively. A $\lambda/8$ shim, which is typically used as a calibration standard, was used to mount the SUEX sample inside the waveguide following a two-port calibration.

The 48 mm diameter, UV-cured and green samples were provided by DJ MicroLaminates, Inc., with 150-μm thickness, as shown in Fig. 2. We prepared the samples by placing two different $\lambda/8$ spacers (one for each band) on a hotplate and green SUEX samples onto waveguide openings. As the hotplate was heated upto 100 °C, the SUEX film started to reflow into the waveguide openings effectively, allowing for a uniform material thickness inside the shim's waveguide section. Upon successful reflow and deposition of SUEX inside the shim, the samples were removed from the hotplate after 1 h cooling step down to room temperature. Subsequently, any residual SUEX on the shim's surface was carefully cleaned using acetone.

As mentioned above, the NRW approach relies on calibrated measurements of two-port S-parameters. Here, we performed a short-open-load-through calibration using the available calibration kit, which consists of three short standards (a standard short, a $\lambda/8$ shim, and a $\lambda/4$ shim) for each port and through the standard between Ports 1 and 2. Subsequently, shims carrying the SUEX samples were carefully inserted between two waveguide sections using the alignment pins and the S-parameters were measured using the VNA.

The analytical model for the NRW approach is based on the assumption of a pure TE_{10} mode in a rectangular waveguide. As such, measured S_{11} is considered as the ratio of the reflected electric field to the incident electric field. Similarly, measured S_{21} is the ratio of the transmitted electric field to the incident electric field. As long as the sample's surface is sufficiently planar and the samples do not have any nonuniformities (such

as air bubbles or other contaminants), the pure TE_{10} assumption would hold and the NRW procedure can be applied. The extraction of permittivity and loss tangent were performed using analytical equations in TE_{10} rectangular waveguide system as follows. First, the measured S-parameters can be expressed as [13]

$$S_{11} = \frac{(1-\Theta^2)\Gamma}{1-\Theta^2\Gamma^2} \quad S_{21} = \frac{(1-\Gamma^2)\Theta}{1-\Theta^2\Gamma^2} \tag{1}$$

where Θ and Γ are the propagation factor and internal reflection coefficient, respectively. The propagation factor and internal reflection coefficient are given by conventional expressions [13]

$$\Theta = \exp(-jk_z d) \quad \Gamma = \frac{\sqrt{\frac{\mu}{\epsilon}} - \sqrt{\frac{\mu_0}{\epsilon_0}}}{\sqrt{\frac{\mu}{\epsilon}} + \sqrt{\frac{\mu_0}{\epsilon_0}}} \tag{2}$$

where k_z is the z-component of propagation vector. Here, we note that $k_0 = \omega\sqrt{\mu_0\epsilon_0}$ is the wavenumber in free space and $k = \omega\sqrt{\mu\epsilon}$ is the unknown wavenumber in the material. Rearrangement of the expressions given in (1) leads to a simple quadratic equation for Γ. Once Γ is determined, Θ is calculated using

$$\Theta = \frac{S_{11} + S_{21} - \Gamma}{1-(S_{11}+S_{21})\Gamma}. \tag{3}$$

Second, k_z is computed by taking the natural logarithm of Θ, using the relation expressed in (2). Finally, the complex permittivity of the sample under test can be calculated using

$$\epsilon_r = \frac{({k_z}^2 + (\frac{\pi}{a})^2)\sqrt{{k_0}^2 - (\frac{\pi}{a})^2}(1-\Gamma)}{k_z {k_0}^2(1+\Gamma)} \tag{4}$$

where a is the longer dimension of the rectangular waveguide.

As mentioned above, the TE_{10} propagation constant k_z for the material-loaded waveguide factors into (1) through the propagation coefficient Θ in (2), as well as the extracted permittivity in (4). It is implicitly determined through (3) from the measured reflection and transmission coefficients.

III. TDS Setup for Permittivity Characterization

To verify the NRW results obtained in Section II, we also characterized the SUEX samples using an independent and completely different approach. A commercial THz-TDS system (TPS Spectra 3000 from TeraView, Inc.) was utilized to obtain the transmission coefficient measurements of the SUEX samples. A 150-μm-thick UV-cured sample and a 200-μm-thick green sample were used for TDS characterization. The measurements were performed in nitrogen-dry environment to eliminate artifacts caused by water vapor and other absorption lines in atmosphere. We also note that (thanks to the quasi-optical system used in the THz TDS) the measured transmission coefficient can be approximated as a plane-wave transmission, as long as the sample's electrical thickness is much smaller than the depth of focus of the THz-TDS system. Subsequently, we fit the analytical formula for the transmission from a thin dielectric layer to the measured data over a wide frequency range. The TDS measurements were performed over the 60-GHz–4-THz band; however, we have only considered the 90-GHz–2-THz data where sufficient signal-to-noise ratio was available. The TDS setup had frequency resolution of 3.59 GHz, where each frequency data was integrated over 300 times to eliminate the random errors from amplitude fluctuations of femtosecond model-locked laser. The THz-TDS tool is a coherent measurement technique, where both amplitude and phase of signal can be recorded. Thus, the loss tangent and dielectric constant can be obtained from the measured complex refractive index by $\epsilon_r = n^2$.

As mentioned above, the multilayered transmission coefficient can be used to construct an analytical model for transmission through a thin film. Namely, the complex transmission coefficient (considering a plane-wave transmission through a single dielectric slab) can be written as [14]

$$\mathcal{T} = \frac{4k_0 k e^{-jkd}}{(k_0+k)^2 - (k_0-k)^2 e^{-2jkd}} \tag{5}$$

where k_0 and k denote the wave numbers in free space and the thin film, respectively. Also, d is the measured sample thickness, which is used as an initial input to the transmission coefficient model given in (5). We note here that the above-mentioned formula assumes a normally-incident plane wave onto a sample that is modeled as an isotropic homogeneous layer. The complex permittivity of the sample is related to complex wavenumber by $k = \omega\sqrt{(\mu_0\epsilon_0\epsilon_r)}$ and the relative complex permittivity is defined as $\epsilon_r = \epsilon_r' - j\epsilon_r''$, where both ϵ_r' and ϵ_r'' are smooth functions of frequency. As in [1], we extracted the frequency-dependent complex permittivity by modeling its real and imaginary parts using second-order polynomials, viz.,

$$\epsilon_r' = \theta_1 + \theta_2 f^2 \tag{6}$$

$$\epsilon_r'' = \theta_3 + \theta_4 f + \theta_5 f^2. \tag{7}$$

Using the above-mentioned analytical model, an iterative nonlinear least-squares method was employed to determine the six real unknowns θ_i in (6) and (7), and the sample thickness d to arrive at the material permittivity and loss over a broad frequency range. We also note that the sample thickness was measured using a micrometer (Mitutoyo Coolant Proof Micrometer Series 293) and was subsequently used as an initial guess for the least-squares procedure. The cost function for the data fitting was defined as

$$\sum_{i=1}^{n} \left(T_{\text{model}}(i) - T_{\text{measured}}(i)\right)^2 \tag{8}$$

where the transmission coefficient magnitudes for the analytical model and measurements are denoted as $T_{\text{model}}(i)$ and $T_{\text{measured}}(i)$, respectively, for ith frequency point.

IV. Results and Discussion

The NRW characterization of green SUEX permittivity and loss tangent are shown in Fig. 3, where two different samples were used to collect the S-parameter measurements in the WR8.0 and WR5.1 bands, covering 90–220 GHz. The solid

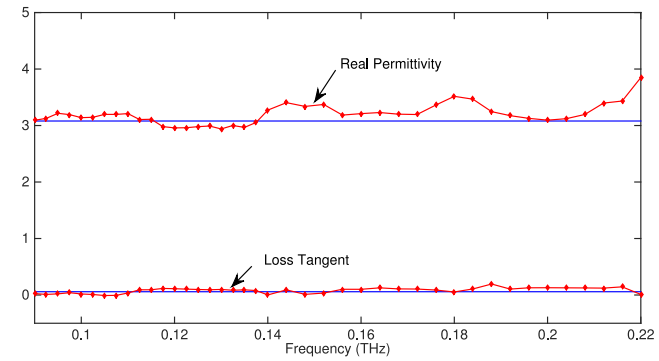

Fig. 3. Measured permittivity and loss tangent of green SUEX using NRW method (solid lines are permittivity and loss tangent values extracted using a THz-TDS system).

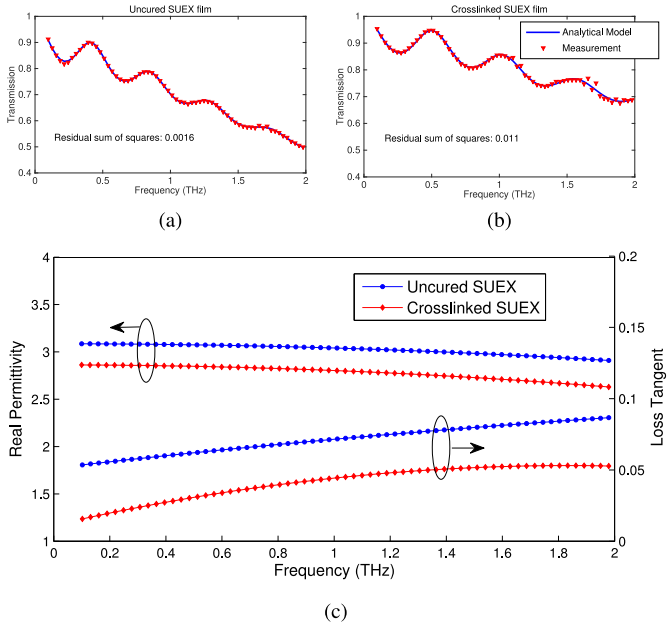

Fig. 4. THz-TDS material characterization of SUEX. (a) Measured and computed transmission amplitude for green SUEX film. (b) Measured and computed transmission amplitude for cured SUEX film. (c) Measured real permittivity and loss tangent as a function of frequency for green and cured SUEX samples.

lines in Fig. 3 indicate the computed values of permittivity and loss tangent using the THz-TDS measurement system. As will be illustrated in Fig. 4, the TDS measurements span a much wider band (90 GHz–2 THz) compared to the waveguide-limited NRW measurements, which relied on an electrically-thin sample ($1/8$th of a wavelength) in our setup. As such, the transmitted waves in the NRW measurements experience little interaction with the electrically thin sample (viz. $1/8$th of a wavelength mid-band), thus, the relative accuracy of the extracted material loss tangent is typically low; whereas the 200-μm-thick samples used in the TDS system are thicker than two wavelengths at 2 THz, which results in substantially longer interaction with the transmitted signals, thus, improving the quality of loss measurements. Here, we note that the NRW method provides a direct extraction of material properties from measurements, whereas

TABLE I
THz-TDS CHARACTERIZATION OF GREEN AND CURED SUEX FILMS

Frequency	*200* GHz	*1* THz	*2* THz
Green SUEX			
Real permittivity	3.08	3.04	2.91
Loss tangent	0.058	0.071	0.087
Cured SUEX			
Real permittivity	2.86	2.80	2.62
Loss tangent	0.020	0.044	0.052

TDS results are extracted through curve fitting the measured data, which relies on a polynomial model given in (6) and (7). The agreement between these two distinct approaches provides confidence that the actual material properties are accurately captured.

THz-TDS characterization results are shown in Fig. 4 for the 90-GHz–2-THz band, using least-squares curve fitting to the measured transmission coefficient. As is evident in both Fig. 4(a) and (b), the loss of the SUEX samples results in a smooth decrease of the transmission amplitude, whereas the finite thickness of the sample results in a periodic ripple as a function of frequency.

For the TDS measurements, we considered both a green (unprocessed) and a fully-cross-linked sample, to illustrate the impact of cross linking on the material parameters. As seen, least-squares method results in an excellent fit to the measurements, where the polynomial approximations (6) and (7) were used for the real and imaginary parts of the permittivity.

Fig. 4(c) depicts the extracted real permittivity and loss tangent results for the 90 GHz–2 THz band. The impact of polymerization can be clearly observed, where the green SUEX film exhibits higher real permittivity and higher material losses, where the permittivity was computed to be at 3.08 at 90 GHz and reduces to 2.91 at 2 THz. For cross-linked SUEX film, the real permittivity ranges from 2.86 down to 2.62, at 90 GHz and 2 THz, respectively. The loss tangent for the cured SUEX film using the TDS approach is 0.015 and 0.052 at 90 GHz and 2 THz, respectively. In comparison, the measurements and analysis indicate a clear difference in the loss properties of uncured versus cross-linked SUEX films, with cross-linked films exhibiting substantially lower electromagnetic loss over all the mmW and THz frequencies measured. This is due to the fact that the THz properties of polymers are affected by the degree of polymerization and the chain length, where the cross-linked polymer chains are tightly bounded to each other with less disorder, leading to lower permittivity and loss tangent.

To demonstrate the uncertainty in the measurements and its impact on the least-squares permittivity and loss tangent re-

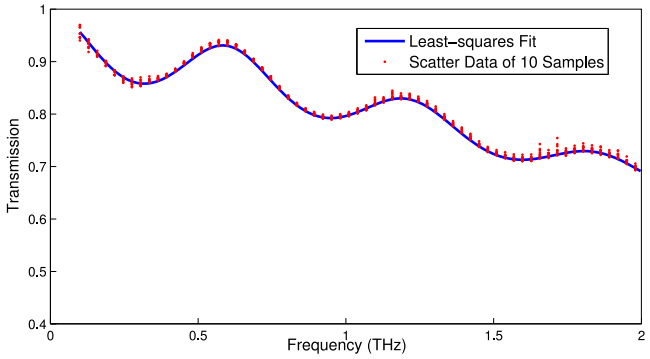

Fig. 5. Transmission amplitude measurements for ten cross-linked SUEX samples (shown as a scatter plot) along with the best analytical fit (solid line).

sults, we considered a set of ten distinct cross-linked SUEX samples. The scatter plot of the measured transmission coefficient is shown in Fig. 5, along with the best least-squares fit curve. To assess the permittivity and loss tangent uncertainty, we applied the least-squares fit to the set of ten samples over the same frequency range. As a result, the calculated permittivity of the samples exhibited $\pm 1.2\%$, $\pm 1\%$, and $\pm 1\%$ at 200 GHz, 1 THz, and 2 THz, respectively. The corresponding uncertainty for the loss tangent was $\pm 9.9\%$ at 200 GHz, $\pm 3.1\%$ at 1 THz, and $\pm 2.4\%$ at 2 THz. We also note that the sample thickness d determined by the least squares fit was within ± 1 μm of the nominal value of 145 μm.

V. Conclusion

We presented a comprehensive characterization of the dielectric properties of SUEX films, using the NRW method, and a commercial THz-TDS system. Particularly, the NRW technique is applied by collecting two-port S-parameter measurements of SUEX samples inside the TE_{10} mode waveguide systems over two successive waveguide bands. Subsequently, the permittivity was analytically extracted from the reflection and transmission measurements via the NRW procedure. In addition, the broadband measurement of the sample's transmission coefficient was used to obtain a polynomial approximation of the material properties over a much larger frequency range using a THz-TDS measurement system. The measured NRW and curve-fitted TDS results are observed to be very consistent with each other. As mentioned above, SUEX permittivity and loss is comparable to the commonly used SU-8, thus, it could prove to be a cost-effective and easy-to-use alternative for mmW and THz applications. The ability to fabricate high-resolution structures with much less effort in process optimization makes SUEX an attractive alternative over traditional liquid photoresists.

References

[1] N. Ghalichechian and K. Sertel, "Permittivity and loss characterization of SU-8 films for mmW and terahertz applications," *IEEE Antennas Wireless Propag. Lett.*, vol. 14, pp. 723–726, 2015.

[2] R. G. Pierce, R. Islam, R. M. Henderson, and A. Blanchard, "SU-8 2000 millimeter wave material characterization," *IEEE Microw. Wireless Compon. Lett.*, vol. 24, no. 6, pp. 427–429, Jun. 2014.

[3] M. Naftaly and R. E. Miles, "Terahertz time-domain spectroscopy for material characterization," *Proc. IEEE*, vol. 95, no. 8, pp. 1658–1665, Aug. 2007.

[4] F. D. Mbairi and H. Hesselbom, "High frequency design and characterization of SU-8 based conductor backed coplanar waveguide transmission lines," in *Proc. IEEE Int. Symp. Adv. Packag. Mater., Processes, Properties Interfaces,* 2005, pp. 243–248.

[5] W. Dai, K. Lian, and W. Wang, "A quantitative study on the adhesion property of cured SU-8 on various metallic surfaces," *Microsyst. Technol.*, vol. 11, no. 7, pp. 526–534, 2005.

[6] R. L. Barber, M. K. Ghantasala, R. Divan, D. C. Mancini, and E. C. Harvey, "Study of stress and adhesion strength in SU-8 resist layers on silicon substrate with different seed layers," *J. Micro/Nanolithography, MEMS, MOEMS*, vol. 6, no. 3, pp. 033 006–033 006, 2007.

[7] M. Nordström *et al.*, "Investigation of the bond strength between the photo-sensitive polymer SU-8 and gold," *Microelectron. Eng.*, vol. 78, pp. 152–157, 2005.

[8] S. Grist, J. N. Patel, M. Haq, B. L. Gray, and B. Kaminska, "Effect of surface treatments/coatings and soft bake profile on surface uniformity and adhesion of SU-8 on a glass substrate," *Proc. SPIEMOEMS-MEMS., Int. Soc. Opt. Photon.*, vol. 7593, 2010, Art. no. 75 930F.

[9] S. Ashraf, C. G. Mattsson, M. Fondell, A. Lindblad, and G. Thungström, "Surface modification of SU-8 for metal/SU-8 adhesion using RF plasma treatment for application in thermopile detectors," *Mater. Res. Express*, vol. 2, no. 8, 2015, Art. no. 08650.

[10] D. W. Johnson, J. Goettert, V. Singh, and D. Yemane, "SUEX process optimization for ultra-thick high-aspect ratio LIGA imaging," *Proc. SPIE*, 2011, Art. no. 79722U.

[11] "SUEX epoxy thick film sheets (TDFS)," DJ MicroLaminates, Sudbury, MA, USA, preliminary data sheet, 2017. [Online]. Available: https://djmicrolaminates.com/datasheets/DJ-MicroLaminates-SUEX-Data-She et-7142017.pdf

[12] D. Johnson, A. Voigt, G. Ahrens, and W. Dai, "Thick epoxy resist sheets for MEMS manufacturing and packaging," in *Proc. IEEE 23rd Int. Conf. Micro Electro Mech. Syst.*, 2010, pp. 412–415.

[13] E. J. Rothwell, J. L. Frasch, S. M. Ellison, P. Chahal, and R. O. Ouedraogo, "Analysis of the Nicolson–Ross–Weir method for characterizing the electromagnetic properties of engineered materials," *Prog. Electromagn. Res.*, vol. 157, pp. 31–47, 2016.

[14] W. C. Chew, *Waves and Fields in Inhomogeneous Media*, vol. 522. Piscataway, NJ, USA: IEEE Press, 1995.

Seckin Sahin (GS'14) was born in Erzincan, Turkey, on November 5, 1990. She received the B.S. degree in electrical and electronics engineering from Bilkent University, Ankara, Turkey, in 2013, the M.S. degree in electrical and computer engineering from The Ohio State University, Columbus, OH, USA, in 2018, and is currently working toward the Ph.D. degree in electrical and computer engineering at The Ohio State University.

She is currently a Graduate Research Associate with the ElectroScience Laboratory, The Ohio State University. Her research interests include microfabrication, ultra-wideband low-profile phased arrays for mobile applications, mmW antenna measurement techniques, and THz spectroscopy systems for material characterization.

Miss. Sahin was the recipient of the Best Student Paper Award of the 2016 IEEE Antennas and Propagation Symposium. In 2018, she was the recipient of the IEEE Antennas and Propagation Society Doctoral Research Grant.

Niru K. Nahar (S'04–M'08–SM'13) received the B.Sc.(Hons.) degree in physics from the University of Dhaka, Dhaka, Bangladesh, the M.S. degree in physics from the Indiana University of Pennsylvania, Indiana, PA, USA, and the M.S. and Ph.D. degrees in electrical and computer engineering from The Ohio State University (OSU), Columbus, OH, USA, in 2002 and 2008, respectively.

She is currently a Research Assistant Professor with the ElectroScience Laboratory, Electrical and Computer Engineering Department, OSU, where she has been a Researcher, since 2008. She is also the Operational Manager of the new HELIOS (THz & mm-Wave) Laboratory, OSU, which was established with the 3.5 million grant from Ohio Third Frontier. She has authored or co-authored 1 book, 1 book chapter, and more than 30 journal papers and 90 conference proceedings and abstracts. She has over three years of research experience in optometry and vision science. She was also a Research Intern with the Surface Analysis Laboratory, Chemical & Metallurgical Division, Osram Sylvania Inc., Towanda, PA, USA. Her current research interests include the designs and characterization of THz and mmW sensors, THz spectroscopy systems for biomedical imaging, mmW ultra-wideband low-profile antennas and phased arrays for cognitive sensing, reconfigurable arrays, novel RF-EO sensors and materials, optical true time delay engines, optical and mmW beam steering, and frequency selective surfaces.

Dr. Nahar is a Senior Member of the Optical Society (OSA) and member of the IEEE Antennas and Propagation Society, the IEEE Lasers and Electro-Optics Society, and OSA. From 2011 to 2014, she was a Secretary/Treasurer, the Vice-Chairman, and the Chairman of the IEEE Joint AP/MTT Chapter Columbus Section. Since 2016, she has been an elected member of URSI Commission B. In 2015, she was the recipient of the Lumley Research Award from the College of Engineering, OSU for her outstanding research.

Kubilay Sertel (M'03–SM'07) received the Ph.D. degree from the Department of Electrical Engineering and Computer Science, University of Michigan–Ann Arbor, Ann Arbor, MI, USA, in 2003.

From 2003 to 2012, he was a Research Scientist with the ElectroScience Laboratory, The Ohio State University, Columbus, OH, USA, where he was also an Adjunct Professor with the Department of Electrical and Computer Engineering. From 2012 to 2017, he was an Assistant Professor. He is currently an Associate Professor with the Electrical and Computer Engineering Department, The Ohio State University. He co-authored *Integral Equation Methods for Electromagnetics* (SciTech Publishing, 2012) and *Frequency Domain Hybrid Finite Element Methods in Electromagnetics* (Morgan & Claypool, 2006), 6 book chapters, 3 patents, and has authored or co-authored more than 80 journal papers and 300 conference papers. His current research interests include the analysis and design of THz and mmW sensors and radars, on-wafer noncontact metrology systems for device and IC testing, biomedical applications of THz imaging, as well as spectroscopy techniques for nondestructive evaluation. His research interests also include ultra-wideband low-profile phased arrays for cognitive sensing and opportunistic wireless networks, reconfigurable antennas and arrays, applied electromagnetic theory, and computational electromagnetics, particularly, curvilinear fast multipole modeling of hybrid integral equation/finite element systems and the efficient solution of large-scale real-life problems on massively parallel supercomputing platforms.

Dr. Sertel is a member of the IEEE Antennas and Propagation Society and the Microwave Theory and Techniques Society and an elected member of URSI Commission B. He is a Fellow of the Applied Computational Electromagnetics Society. He is also the Editor-in-Chief for the IEEE Antennas and Propagation Society.